A *priori* testing of subgrid-scale models for a two-phase turbulent flow: Droplets in Homogeneous-Isotropic Turbulence

Suhas S Jain, Sanjiva K Lele

February 17, 2018

Abstract

A priori testing (Clark et al. 1979) is very important in analyzing the performance of the subgrid-scale (SGS) models in the LES calculation of turbulent flows. Detailed analysis of this sort is still lacking in the literature for some canonical two-phase turbulent flow problems. So, the aim of this project is to perform *a priori* testing to study the order of magnitude of different unclosed terms and to evaluate the performance of sub-grid models for the LES of flow of droplets in a homogeneous-isotropic turbulence (HIT) in a triply-periodic box.

1   Introduction

In a typical *a priori* test, governing equations of the flow are filtered and the unclosed terms are derived. Order of magnitude of these unclosed terms are estimated and compared, to choose the dominating unclosed term that introduces the most-significant error. The prediction from the chosen sub-grid models for these unclosed terms are compared against the computed values from the DNS data to evaluate the performance of the sub-grid models in LES setting.

Additionally, *a priori* testing can also be done with different filters and filter sizes, and the effect of these parameters on the unclosed terms can be studied to get an insight on choosing the best filter and filter size for the problem being studied.

In the current study, we use the available DNS data for a gas-liquid system at $Re = 6.42 \times 10^4$, $We = 1.53 \times 10^4$. There are 3130 Taylor length scale size droplets ($D \approx \lambda$) in a decaying HIT in a triply-periodic box. Other relevant non-dimensional parameters are density ratio = 10, viscosity ratio = 10 and $We_{rms} = 1$. The turbulent flow is well resolved on a $1024 \times 1024 \times 1024$ grid with ≈ 32 grid points per diameter of the drops. A snapshot of the simulation can be seen in the Figure 1. For more information on these simulations, see, (Dodd & Ferrante 2016).
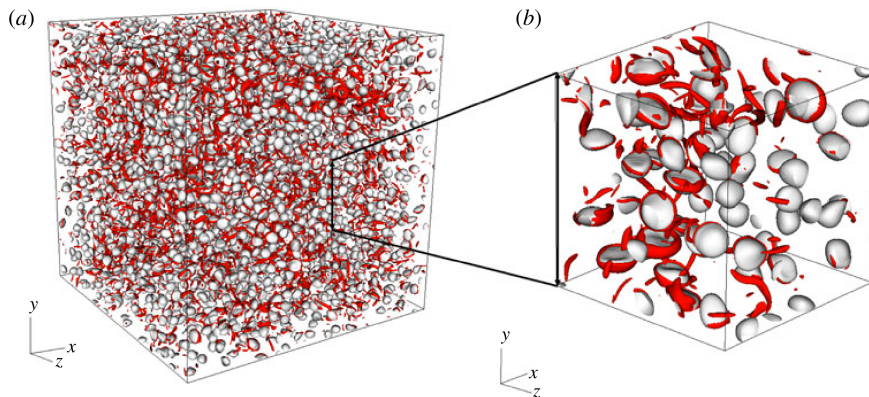

Figure 1: Snapshot of the DNS of droplets in HIT from Figure 3 of Dodd & Ferrante (2016) showing the drops and vorticity isosurfaces.

2   Formulation

This section describes the unfiltered governing equations for two-phase flows based on both "one-fluid" and "two-fluid" formulation. We choose "one-fluid" formulation for our study and hence the filtered equations and the unclosed terms based on "one-fluid" formulation are also described in this section. A more detailed derivation of these can be found in the Appendix **A**.

2.1   Unfiltered equations

Consider a sharp-massless interface represented by an implicit function f, where $f^k(\vec{x}, t) = 0$ represents the location of the interface, $\vec{x}$ belongs to k^{th} phase if $f^k(\vec{x}, t) > 0$. Additionally, a sharp phase-indicator function χ^k can be defined as $\chi^k = H(f^k)$, where H is the Heaviside function. Then, the governing equations for the conservation of the mass can be written as,

$$\frac{\partial \chi^k \rho^k}{\partial t} + \vec{\nabla} \cdot (\chi^k \rho^k \vec{u}^k) = \rho^k (\vec{W} - \vec{u}^k) \cdot \vec{n}^k \delta_i, \tag{1}$$

where $\vec{W}$ represents the interface velocity, δ_i represents the surface diract delta function, and hence the term on the RHS is the source/sink due to mass transfer across the interface. Governing equations for the conservation of momentum can be written as,

$$\frac{\partial \chi^k \rho^k \vec{u}^k}{\partial t} + \vec{\nabla} \cdot [\chi^k (\rho^k \vec{u}^k \otimes \vec{u}^k + p^k \mathbb{1} - \underline{\underline{\tau}}^k)] - \chi^k \rho^k g = [\rho^k \vec{u}^k \otimes (\vec{W}^k - \vec{u}^k) + p^k \mathbb{1} - \underline{\underline{\tau}}^k] \cdot \vec{n}^k \delta_i, \tag{2}$$

where the term on the RHS is the source/sink of the momentum flux across the interface due to mass transfer and pressure and shear stresses acting at the interface.

A one-fluid variable ϕ can be defined as $\phi = \sum_k \chi^k \phi^k$. Summing the equation 1 for all the phases and replacing the RHS term by an interface jump condition, we get conservation of mass based on one-fluid formulation as,

$$\frac{\partial \rho}{\partial t} + \vec{\nabla} \cdot (\rho \vec{u}) = 0. \tag{3}$$

Similarly, the conservation of momentum for one-fluid formulation can be derived by summing the equation 2 for all the phases and replacing the RHS term by an interface jump condition as,

$$\frac{\partial \rho \vec{u}}{\partial t} + \vec{\nabla} \cdot (\rho \vec{u} \otimes \vec{u} + p \mathbb{1} - \underline{\underline{\tau}}) - \rho g = [\sigma \vec{n}^k (\nabla_s \cdot \vec{n}^k) - \nabla_s \sigma] \delta_i, \tag{4}$$

where ∇_s represents the surface derivative operator and σ is the surface tension.

2.2   Filtered equations

Filtering for the variable u is defined as the convolution of u with a suitable kernel G as,

$$\overline{u(\vec{x}, t)} = \int_{-\infty}^{t} \int_{\Omega} G(\overline{\Delta}, \vec{x} - \vec{x'}, t - t') u(\vec{x'}) dx' dt', \tag{5}$$

where $\overline{\Delta}$ is the cut-off length scale. Since the density is varying in space, Favre average defined as, $\widetilde{u} = \overline{\rho u} / \overline{u}$ is used. Applying this filtering to Equations 3 and 4 gives the Favre averaged filtered set of equations for one-fluid formulation with exact jump conditions as,

$$\frac{\partial \overline{\rho}}{\partial t} + \vec{\nabla} \cdot (\overline{\rho} \widetilde{u}) = 0. \tag{6}$$

$$\frac{\partial \overline{\rho} \widetilde{u}}{\partial t} + \vec{\nabla} \cdot (\overline{\rho} \widetilde{u} \otimes \widetilde{u} + \overline{p} \mathbb{1} - \overline{\mu S_D}) + \underline{\underline{\tau}}_{fl_{\rho u u}} + \underline{\underline{\tau}}_{fl_{\mu S}} = [\overline{\sigma}^s \overline{\vec{n}}^s \overline{(\nabla_s \cdot \vec{n})}^s - \overline{\nabla_s}^s \overline{\sigma}^s] \overline{\delta_i} + \underline{\underline{\tau}}_{r_{\sigma n}} + \underline{\underline{\tau}}_{r_{\sigma t}}, \tag{7}$$

where surface filtering $\overline{\phi}^s$ is defined as,

$$\overline{\phi}^s = \frac{\int_{\Omega} \delta_i \phi d\vec{x}}{\int_{\Omega} \delta d\vec{x}} = \frac{\overline{\delta_i \phi}}{\overline{\delta_i}} \tag{8}$$

2.3 Assumptions

We further make few assumptions that simplifies our analysis:

- Only two phases.

- Incompressible fluids, hence ρ is constant in each phase.

- No mass transfer.

- Isothermal and no chemical reactions, hence μ is constant in each phase and σ is constant.

- No sliding between the phases, hence filtering and gradient operators commute.

- Immiscible fluids.

2.4 Unclosed terms

Making the simplifications based on the assumptions listed in the previous section, we are left with three unclosed terms in the Equation 7 that requires modeling. The three unclosed terms are convective, viscous and interfacial tension terms given by,

$$\underline{\underline{\tau}}_{fl_{\rho uu}} = \overline{\rho \vec{u} \otimes \vec{u}} - \overline{\rho}\widetilde{\vec{u}} \otimes \widetilde{\vec{u}} \tag{9}$$

$$\underline{\underline{\tau}}_{fl_{\mu S}} = \overline{\mu S_D} - \overline{\mu}\widetilde{S_D} \tag{10}$$

$$\underline{\underline{\tau}}_{r_{\sigma n}} = \overline{\delta_i \vec{n}(\nabla_s \cdot \vec{n})} - \overline{\delta_i}\ \overline{\vec{n}}^s\overline{(\nabla_s \cdot \vec{n})}^s \tag{11}$$

For full expansion of these terms in three dimensions, see Appendix **B**.

3 Order of magnitude analysis

Relative importance of each of the unclosed terms depend on the problem being studied. Hence, we estimated the magnitude of each of the unclosed terms for our test case of HIT in the presence of droplets. For the case of phase inversion in a closed box, see, Vincent et al. (2008) and Labourasse et al. (2007) and for a single bubble in HIT, see, Toutant et al. (2006)).

3.1 Filters and filter sizes

Since the drops are of $\approx 32\Delta x$ in diameter, we used five filter sizes $\overline{\Delta} = 2\Delta x, 4\Delta x, 16\Delta x, 32\Delta x$ and $64\Delta x$ to study the effect of filter size on the interfacial structures that are of $\approx 32\Delta x$ in size. When, $\overline{\Delta} < 32\Delta x$, it represents a regime where the drops are still resolved by the LES grid, when $\overline{\Delta} = 32\Delta x$, it represents the regime where the drops are of approximately the same size as of the LES grid and when $\overline{\Delta} > 32\Delta x$, it represents a regime where the drops are fully sub-grid.

We filter the fields in frequency space, due to the increasingly expensive filtering process with increasing filter sizes in physical space. We estimated that the filtering in the physical space for the data we have takes $\approx 1day$ on a single node of Stampede2 supercomputer for a filter size of $\overline{\Delta} = 4\Delta x$ and hence was not feasible for larger filter sizes. However, filtering in the frequency space, takes $\approx 10min$, given the available memory is large enough $> \approx 150GB$.

To filter our data, we choose two kernels spectrally sharp and Gaussian given by,

$$G_{sharp} = \begin{cases} 1 & nk\Delta x < \pi/2 \\ 0 & else. \end{cases} \tag{12}$$

$$G_{gauss} = exp\Big[- \frac{(nk\Delta x)^2}{4} \Big], \tag{13}$$

where n is the filter factor. The corresponding filter factors for filter sizes of $\overline{\Delta} = 2\Delta x, 4\Delta x, 16\Delta x, 32\Delta x$ and $64\Delta x$ are $n = 1, 2, 8, 16$ and 32.

Classification of the terms in the momentum equation for different filtering sizes

Category	FiSm	FiAv	FiLa	FiHu
Large	$\nabla \cdot \rho u \otimes u + p$	$\nabla \cdot \rho u \otimes u + p$ $\nabla \cdot \tau_{l\rho uu}$	$\nabla \cdot \rho u \otimes u + p$ $\nabla \cdot \tau_{l\rho uu}$	$\nabla \cdot \rho u \otimes u + p$ $\nabla \cdot \tau_{l\rho uu}$
Medium	$\nabla \cdot \tau_{l\rho uu}$ $\nabla \cdot \bar\tau$	$\boxed{\frac{\partial \tau_{l\rho u}}{\partial t}}$	$\boxed{\frac{\partial \tau_{l\rho u}}{\partial t}}$	
Small	$\boxed{\frac{\partial \tau_{l\rho u}}{\partial t}}$ $\nabla \cdot \tau_{l\mu S}$	$\nabla \cdot \bar\tau$ $\nabla \cdot \tau_{l\mu S}$	$\nabla \cdot \bar\tau$ $\nabla \cdot \tau_{l\mu S}$ τ_{rnn}	$\nabla \cdot \bar\tau$ $\nabla \cdot \tau_{l\mu S}$
Negligible	τ_{rnn}	τ_{rnn}		$\boxed{\begin{array}{c}\tau_{rnn}\\ \frac{\partial \tau_{l\rho u}}{\partial t}\end{array}}$

Figure 2: Table 4 from Labourasse et al. (2007) showing the order of magnitude of convective, shear and surface tension unclosed terms for filter sizes $FiSm = 2\Delta x$, $FiAv = 10\Delta x$, $FiLa = 20\Delta x$ and $FiSm = 100\Delta x$, using the DNS data of phase inversion in a closed box on 512×512 grid.
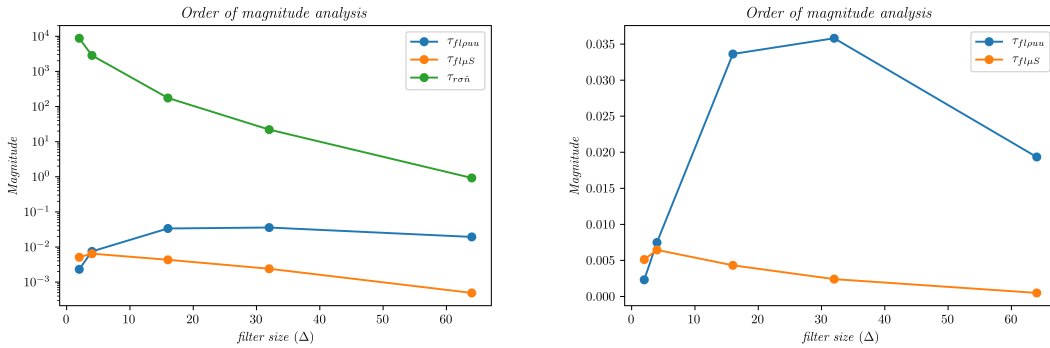

Figure 3: Order of magnitudes of convective $< |\vec\nabla \cdot \underline{\underline{\tau}}_{fl_{\rho uu}}| >$, viscous $< |\vec\nabla \cdot \underline{\underline{\tau}}_{fl_{\mu S}}| >$ and surface tension unclosed terms $< |\underline{\underline{\tau}}_{r_{\sigma n}}| >$ using a Gaussian kernel, where $<>$ denotes a spatial mean.

3.2   Previous studies

Previous studies by Vincent et al. (2008), Toutant et al. (2006), Labourasse et al. (2007) and McCaslin & Desjardins (2014) can be summarized as,

- Convective tensor $\underline{\underline{\tau}}_{fl_{\rho uu}}$ increases with the filter size.

- Shear stress tensor $\underline{\underline{\tau}}_{fl_{\mu S}}$ is small for all filter sizes.

- Surface tension tensor $\underline{\underline{\tau}}_{r_{\sigma n}}$ is very small and decreases with the filter size, since the sub-grid error cancels out due to symmetry as the filter size increases and includes more sub-grid contributions.

Figure 2 shows the order of magnitudes of convective, shear and surface tension unclosed terms for filter sizes $FiSm = 2\Delta x$, $FiAv = 10\Delta x$, $FiLa = 20\Delta x$ and $FiSm = 100\Delta x$, performed by Labourasse et al. (2007) using the DNS data of phase inversion in a closed box on a 512×512 grid.

3.3   Present study

We performed a separate order of magnitude analyses for each of the filters we choose. Figure 3 shows the order of magnitudes for the convective $< |\vec\nabla \cdot \underline{\underline{\tau}}_{fl_{\rho uu}}| >$, viscous $< |\vec\nabla \cdot \underline{\underline{\tau}}_{fl_{\mu S}}| >$ and surface tension unclosed terms $< |\underline{\underline{\tau}}_{r_{\sigma n}}| >$, filtered using a Gaussian kernel, where $<>$ denotes a spatial mean.

Clearly, in the present study the surface tension unclosed term dominates over the other two, which was not seen in the previous studies. It is to be noted that the previous studies Vincent et al. (2008), Toutant et al. (2006), Labourasse et al. (2007) and McCaslin & Desjardins (2014) use volume filtering for the surface tension unclosed terms. However, McCaslin & Desjardins (2014)
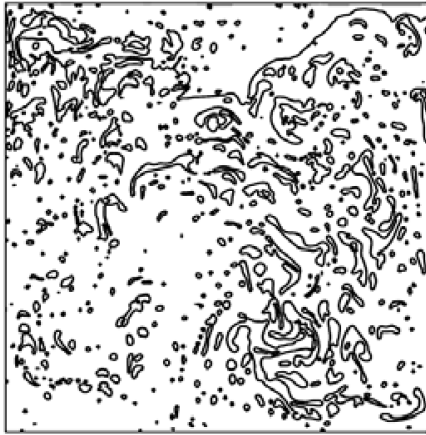
Figure 4: Wide range of interfacial scales seen in the case of phase inversion in a closed box from Figure 8 of Labourasse et al. (2007).
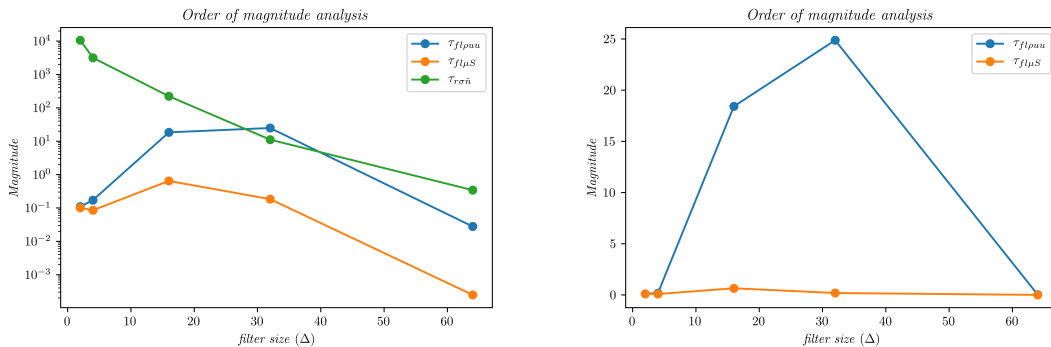

Figure 5: Order of magnitudes of convective $< |\vec{\nabla} \cdot \underline{\underline{\tau}}_{fl_{\rho uu}}| >$, viscous $< |\vec{\nabla} \cdot \underline{\underline{\tau}}_{fl_{\mu S}}| >$ and surface tension unclosed terms $< |\underline{\underline{\tau}}_{r_{\sigma n}}| >$ using a spectrally sharp kernel, where $<>$ denotes a spatial mean.

pointed out that the use of volumetric filtering underpredicts the surface tension unclosed term. So we used a suitable surface kernel to filter the surface tension unclosed terms in our study. Since the surface filtering uses a Dirac delta function to consider only the locations of the interface, error due to the unclosed term is significantly higher because the location of the interface typically changes when the phase indicator function is filtered. This explains the relatively higher magnitude of the surface tension unclosed terms, that we observe.

Second significant term in our study is the convective term. In our case, as we increase the filter size, we see that the convective term increases for the filter sizes $\overline{\Delta} < 32\Delta x$ and then decrease for $\overline{\Delta} > 32\Delta x$. This clearly shows the dependence of the magnitude of the unclosed term on the physical interfacial scales present in the simulation i.e., the drop size of $\approx 32\Delta x$. However, this was not observed in the previous studies because the test cases considered by the previous studies contained a wide range of physical interfacial scales (see, Figure 4). The third and the least significant term is the viscous term that is small for all the filter sizes and this is consistent with the previous observations.

Figure 5 shows a similar trend using a spectrally sharp kernel for the filtering, however the magnitudes are higher when compared to the Gaussian kernel. Further study is required to reason out this observation.

4 Sub-grid model performance evaluation

To the best of our knowledge, we do not know of any previous studies that model the unclosed surface tension terms. Among the convective and viscous terms, since the convective term is

dominant, Vincent et al. (2008), Toutant et al. (2006) and Labourasse et al. (2007) chose to perform *a priori* testing only on the convective term. All these studies, computed an equivalent eddy viscosity given by,

$$\mu_{ef} = \frac{\underline{\underline{\tau}}_{fl_{\rho uu}} : \vec{\nabla}\vec{u}}{S : \vec{\nabla}\vec{u}} \tag{14}$$

and found that the μ_{ef} is negative in some regions and positive in other regions around the interface and concluded that the eddy-viscosity type models are inadequate. Hence they choose a mixed Bardina-Smagorinsky model for their *a priori* tests. Decomposing two variables ϕ and ψ,

$$\overline{\phi\psi} - \overline{\phi}\,\overline{\psi} = L + C + R, \tag{15}$$

where,

$$L = \overline{\overline{\phi}\,\overline{\psi}} - \overline{\overline{\phi}}\,\overline{\overline{\psi}} \tag{16}$$

$$C = \overline{\overline{\phi}\,\psi'} - \overline{\overline{\phi}}\,\overline{\psi'} + \overline{\phi'\,\overline{\psi}} - \overline{\psi'}\,\overline{\overline{\psi}} \tag{17}$$

$$R = \overline{\phi'\,\psi'} - \overline{\phi'}\,\overline{\psi'} \tag{18}$$

L is modeled based on scale-similarity hypothesis and $C+R$ is modeled based on eddy-viscosity hypothesis. Further, following Toutant et al. (2006) we choose to consider only the L term in our study, however in an actual LES simulation, diffusion is required to stabilize the solver. Hence the model can be defined as,

$$\underline{\underline{\tau}}_{fl_{\rho uu}} = \overline{\widetilde{\rho\vec{u}} \otimes \widetilde{\vec{u}}} - \overline{\widetilde{\overline{\rho\vec{u}}}} \otimes \widetilde{\overline{\vec{u}}}, \tag{19}$$

where,

$$\widetilde{\overline{\vec{u}}} = \frac{\overline{\rho\vec{u}}}{\overline{\overline{\overline{\vec{u}}}}}. \tag{20}$$

Using this model, we compute the correlation coefficients as defined in Clark et al. (1979) separately for each of the filter we used. Figure 6 shows the correlation coefficient as a function of filter size for a Gaussian kernel and spectrally sharp kernel. Correlation coefficient for Gaussian kernel on an average is ≈ 0.87, which is very close to what was reported in previous studies about 0.8 for a top-hat kernel. However, one has to be careful in interpreting the high correlation coefficient obtained using sharp kernel. Interestingly, the correlation coefficient decreases for filter size $\overline{\Delta} > 32\Delta x$. We can explain this by looking back at the "scale-similarity hypothesis". This hypothesis says that the structure of the sub-grid scales are similar to the smallest resolved scales because of the cascade process. Therefore, in our case, when the filter size is $\overline{\Delta} > 32\Delta x$, all the interfacial scales are sub-grid and we do not have any interfacial scales that are resolved. Hence the model prediction is not as good as when the filter size $\overline{\Delta} < 32\Delta x$.

Additionally, we also plotted the convective term $< |\vec{\nabla} \cdot \underline{\underline{\tau}}_{fl_{\rho uu}}| >$ along a central horizontal spatial plane and compared it with the plot obtained using the model for all the filter sizes. Overall, the model faithfully reproduces the convective unclosed tensor. See Appendix **C** for the plots.

5   Summary and Conclusion

We here, perform *a priori* testing to analyze the performance of the subgrid-scale (SGS) model in the LES calculation of two-phase turbulent flows. We chose to study the droplets in a homogeneous-isotropic turbulence in a triply-periodic box. We derived the filtered governing equations for two-phase turbulent flows based on "one-fluid formulation" and recognized the convective, viscous and surface tension unclosed terms that require modeling. We performed the order of magnitude analysis of these terms for different filters and filter sizes and found that the magnitude of the convective term is dependent on the physical interfacial scales in the flow. Further following the analysis of Labourasse et al. (2007) and Toutant et al. (2006), we chose to use scale-similarity model and computed the correlation coefficients and concluded that this model faithfully predicts the unclosed convective terms.

Overall, *a priori* tests gave us insights on choosing a filter and filter size, and the choice of the model for the study of LES of two-phase turbulent flows.
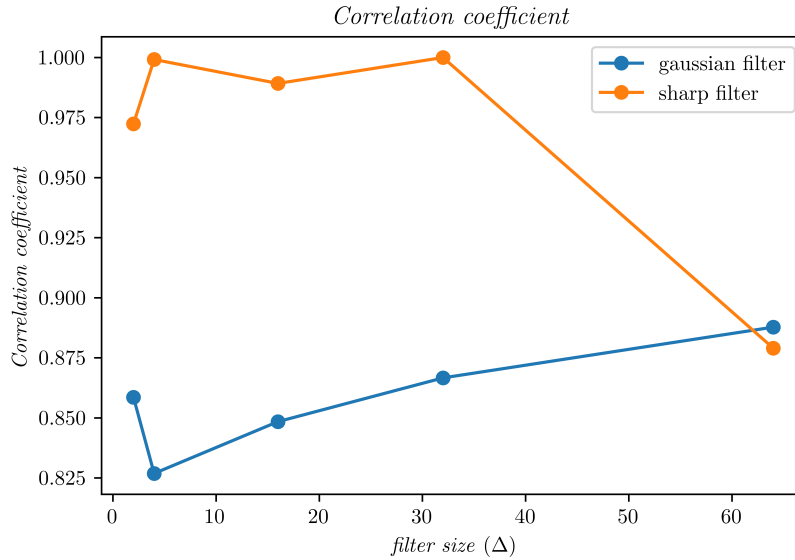
Figure 6: Correlation coefficients for scale-similarity model based on Gaussian kernel and spectrally sharp kernel.

Acknowledgements

References

Clark, R. A., Ferziger, J. H. & Reynolds, W. C. (1979), 'Evaluation of subgrid-scale models using an accurately simulated turbulent flow', *Journal of Fluid Mechanics* **91**(1), 1–16.

Dodd, M. S. & Ferrante, A. (2016), 'On the interaction of taylor length scale size droplets and isotropic turbulence', *Journal of Fluid Mechanics* **806**, 356–412.

Labourasse, E., Lacanette, D., Toutant, A., Lubin, P., Vincent, S., Lebaigue, O., Caltagirone, J.-P. & Sagaut, P. (2007), 'Towards large eddy simulation of isothermal two-phase flows: Governing equations and a priori tests', *International Journal of Multiphase Flow* **33**(1), 1 – 39.
URL: *http://www.sciencedirect.com/science/article/pii/S0301932206000905*

McCaslin, J. O. & Desjardins, O. (2014), 'Theoretical and computational modeling of turbulence/interface interactions', *Center for Turbulence Research, Proceedings of the Summer Program* pp. 79–88.

Toutant, A., Labourasse, E., Lebaigue, O, D. & Simonin, O. (2006), Interaction between a deformable buoyant bubble and a homogenous isotropic turbulence, *in* 'Conference Turbulence and Interactions'.

Vincent, S., Larocque, J., Lacanette, D., Toutant, A., Lubin, P. & Sagaut, P. (2008), 'Numerical simulation of phase separation and a priori two-phase les filtering', *Computers & Fluids* **37**(7), 898 – 906. Special Issue of the "Turbulence and Interaction-TI2006" Conference.
URL: *http://www.sciencedirect.com/science/article/pii/S0045793007001569*